Robust CIECAM02 Implementation and Numerical Experiment within an ICC Workflow

Chunghui Kuo, Eric Zeise and Di Lai; Eastman Kodak, Rochester, NY, USA

Abstract

*CIECAM02 has gained significant interest within the field of color management for its potential in achieving uniform perceptual color space. However, researchers have identified difficulties in adopting CIECAM02 directly in an ICC workflow as the profile connection space, **PCS**, because of the nonlinear post-adaptation response functions as well as the perceptual characteristic functions. In this paper, we will address the slight inconsistency in the CIECAM02 derivation under complete illumination adaptation, and a minimized modification on the Hunt-Pointer-Estevez transformation is derived to overcome this difficulty. Furthermore, a robust computation procedure will be suggested to alleviate certain singularities occurring in the original numerical implementation. Finally, we will verify our proposed implementation and compare with the standard procedure within the scheme of the ICC workflow.*

Introduction

A color appearance model correctly predicting all of the perceptual color attributes, such as hue, brightness, and chroma, is still being actively pursued by many scientists and engineers to be able to better communicate visual perception with one another [1]. With the current rapid advances in image capture and display technologies, such a model is even more critical to ensure the inter-operability among all equipment. The current international standard supported by the *International Color Consortium*, ICC, is the latest effort to standardize the color communication specification [2]. In the ICC specification, a color space, denoted as the *Profile Connection Space*, PCS, is selected from *CIELAB* or *XYZ*, and each imaging system is described by a color profile in the PCS. The PCS is responsible to connect two different imaging systems: one input device and one output device.

Various color appearance models have been proposed over the years, such as *CIELAB*, the Hunt model, the RLAB model, and the latest CIECAM97s and CIECAM02 models [1]. CIECAM02 is considered to successfully accomplish two objectives: ease of use and offering comprehensive predictions of all attributes of color perception [3]. One advantage of adopting CIECAM02 over CIELAB is that the predicted hue angle is better aligned with the perceived hue than that predicted by CIELAB, especially in the blue color region [4]. However, because of the adopted nonlinear post-adaptation function and nonrational definitions of perceived color attributes, researchers have identified several scenarios where the forward and backward algorithms suggested by the CIECAM02 will create numerical irregularities [5, 6]. As a result, special care has to be taken before adopting CIECAM02 directly into the future ICC workflow [7, 8].

In this paper, we will address two issues encountered when adopting CIECAM02 in an ICC workflow: white point under the assumption of complete illumination adaptation, and a numerically robust backward CIECAM02 model. First, although the CIECAM02 suggests a formula to estimate the degree of adaptation, **D**, complete illumination adaptation is usually the preferred choice in the current image reproduction workflow. However, under the current Hunt-Pointer-Estevez transformation defined in CIECAM02, the adapted white point under complete illumination adaptation assumption will not result in the estimated chroma being zero, even though it is very small. Impose the aforementioned constrain of zero chroma, and we will suggest a modified formulation of the Hunt-Pointer-Estevez transformation matrix with minimized impact as a simple quadratic optimization with linear constraints. However, the standard CIECAM02 inverse model has a numerical singularity when converting a point with chroma being zero to XYZ. Although this numerical singularity can be avoided by forcing $a = b = 0$ at $C = 0$, there might still exist difficulties for chroma being very small. This problem is addressed by rearranging the sequence of the backward model.

It is possible to rearrange the sequence of the CIECAM02 backward model without computing a, b, and obtain $R_a^{'}, G_a^{'}, B_a^{'}$ directly via solving a system of linear equations. We will show that, although mathematically equivalent, this algorithm is more robust numerically by adopting the truncated Singular Value Decomposition algorithm, *TSVD*, in solving the 3×3 linear system including the colors with zero chroma [9]. To verify if it is possible to extend the current PCS in an ICC workflow to include CIECAM02, we verify our proposed algorithm in two different routes: $CIELAB(XYZ) \rightarrow CIECAM02 \rightarrow CIELAB(XYZ)$ and $CIECAM02 \rightarrow XYZ(CIELAB) \rightarrow CIECAM02$. In both cases, the initial color spaces are sampled uniformly and form two three-dimensional cubic grids. The first case starts from the set of non-imaginary colors and identifies the necessary and sufficient conditions for the validity of the CIECAM02 numerical model, but the second case will test the robustness of an inverse model with respect to imaginary colors. We will compare two output gamuts via the standard algorithm and our proposed algorithm.

Proposed Implementation

The chromatic adaptation algorithm adopted in the CIECAM02 is a generalized form of the *von Kries* transformation. The tristimulus values are first mapped to RGB responses using the matrix transformation, M_{CAT02}. Denote the cone responses as R, G, B, and the degree of adaptation as D. It can be easily shown that the RGB responses after chromatic adaptation, R_{cw}, G_{cw}, B_{cw}, of the adapted white point under complete illumination adaptation assumption, i.e. $D = 1$, is $(100, 100, 100)$. The adapted tristimulus values are then mapped to the optimized cone

responses via the Hunt-Pointer-Estevez matrix transformation:

$$M_{HPE} = \begin{pmatrix} 0.38971 & 0.68898 & -0.07868 \\ -0.22981 & 1.18340 & 0.04641 \\ 0 & 0 & 1 \end{pmatrix}. \quad (1)$$

The resulting adapted cone responses of the adapted white point, R'_w, G'_w, B'_w is $(100.00001, 100, 100)$. This will result in nonzero opponent-type responses, a and b, of which chroma is nonzero. Since M_{HPE} optimizes the transformation from tristimulus values to cone responses, our objective is to minimize the modification of M_{HPE}, denoted as δM_{HPE}, while satisfying the constraint of zero chroma. It is obvious that the last two rows of δM_{HPE} are zeros; thus, we can postulate δM_{HPE} to be the following:

$$\delta M_{HPE} = \begin{pmatrix} k_1 & k_2 & k_3 \\ 0 & 0 & 0 \\ 0 & 0 & 0 \end{pmatrix}. \quad (2)$$

Adopting $\|\delta M_{HPE}\|^2 = (k_1^2 + k_2^2 + k_3^2)$ as the cost function quantifying the amount of modification, the the modification of M_{HPE} can be reformulated as a simple quadratic programming problem as follows:

$$\begin{aligned} & \min \quad k_1^2 + k_2^2 + k_3^2 \quad (3) \\ s.t. \quad & k_1 + k_2 + k_3 = 0.00001 \\ & k_1, k_2, k_3 \geq 0. \end{aligned}$$

The solution is $(\frac{10^{-5}}{3}, \frac{10^{-5}}{3}, \frac{10^{-5}}{3})$. By limiting to one extra decimal digit, we propose to modify the Hunt-Pointer-Estevez matrix transformation to be the following:

$$\bar{M}_{HPE} = \begin{pmatrix} 0.389707 & 0.688977 & -0.078684 \\ -0.22981 & 1.18340 & 0.04641 \\ 0 & 0 & 1 \end{pmatrix}. \quad (4)$$

Note that $\bar{M}_{HPE} \rightarrow M_{HPE}$ if they are rounded to the fifth decimal point, and $(a,b) = (0,0) = (a_c, b_c)$ for the adapted white point under complete illumination adaptation if $\bar{M}_{HPE}$ is adopted in the forward CIECAM02 model.

One numerical singularity that exists in the standard CIECAM02 backward model is that it is necessary to compute the parameter, P_1, as follows:

$$t = (\frac{C}{\sqrt{J/100}(1.64 - 0.29^n)^{0.73}})^{10/9} \quad (5)$$

$$P_1 = \frac{(50000/13) N_c N_{cb} e_t}{t}, \quad (6)$$

where C and J are chroma and lightness respectively. As a result, if $C = 0$, $P_1 \rightarrow \infty$, and it becomes a singular point [5]. Instead of first solving a and b as suggested by the standard CIECAM02 inverse model, we propose to solve R'_a, G'_a, B'_a directly as explained below. Assuming J, C and h are known, we can first compute the brightness, A, where $A = A_w (J/100)^{1/cz}$. Note that n, N_c, N_{cb} , c and z are internal parameters specified in CIECAM02, and they are assumed to be known a priori [1, 3]. Thus, we can construct the first linear equation:

$$2R'_a + G'_a + \frac{1}{20} B'_a = \frac{A}{N_{bb}} + 0.305. \quad (7)$$

Furthermore, because $\sqrt{a^2 + b^2} = a\sec(h) = b\csc(h)$, we can formulate the second linear equation as follows:

$$\begin{aligned} t(R'_a + G'_a + \frac{21}{20} B'_a) &= ((50000/13) N_c N_{cb} e_t \sec(h)) a \\ &= P_2 (R'_a - \frac{12}{11} G'_a + \frac{1}{11} B'_a) \quad (8) \\ &= ((50000/13) N_c N_{cb} e_t \csc(h)) b \\ &= \bar{P}_2 (R'_a + G'_a - 2B'_a). \quad (9) \end{aligned}$$

At last, based on $\tan(h) = \frac{b}{a}$, the last equation can be easily constructed:

$$\tan(h)(R'_a - \frac{12}{11} G'_a + \frac{1}{11} B'_a) = \frac{1}{9}(R'_a + G'_a - 2B'_a) \quad (10)$$

$$\frac{\cot(h)}{9}(R'_a + G'_a - 2B'_a) = (R'_a - \frac{12}{11} G'_a + \frac{1}{11} B'_a). \quad (11)$$

Only one equation in the last two cases is selected depending on the relationship between $|\sin(h)|$ and $|\cos(h)|$. If $|\sin(h)| \leq |\cos(h)|$, $\tan(h)$ and $\sec(h)$ are chosen. Otherwise, $\cot(h)$ and $\csc(h)$ are selected. As a result, a 3×3 linear system with R'_a, G'_a, B'_a being three unknowns can be constructed, and solved via the *TSVD* algorithm [9]. In the case of $C = 0$, the linear system can be simplified to be following:

$$\begin{bmatrix} 2 & 1 & 1/20 \\ 1 & -12/11 & 1/11 \\ 1/9 & 1/9 & 1/9 \end{bmatrix} \begin{bmatrix} R'_a \\ G'_a \\ B'_a \end{bmatrix} = \begin{bmatrix} \frac{A}{N_{bb}} + 0.305 \\ 0 \\ 0 \end{bmatrix}. \quad (12)$$

The singular values of the 3×3 matrix are 2.1, 1.39 and 0.11, and its condition number is 20.9. This indicates that it is a well-posed least square problem, and can be solved reliably. As a result, the singularity caused by the standard CIECAM02 inverse model in computing P_1 can be avoided by adopting our proposed approach. The other advantage of solving a least square problem is that, if the singular values of the resulting 3×3 matrix become too small, the corresponding singular vectors can be treated as the null space and removed from the solution.

Numerical Experiment

We propose two possibilities for including CIECAM02 into an ICC workflow:

Case 1 PCS remains CIELAB space(or XYZ).
Case 2 CIECAM02 becomes one of the choices for PCS.

In the first case, CIECAM02 is only used to perform gamut mapping, but the final realization is represented in the CIELAB space (or XYZ). Thus, it is necessary to verify the color space transformation from CIELAB to CIECAM02 and back to CIELAB. In the second case, the CIECAM02 color space is sampled by a three-dimensional grid similar to the current ICC PCS implementation. Thus, it is also imperative to identify the region of physically feasible colors within the sampling grid. Moreover, the current profile accuracy estimation is obtained by comparing the color difference between one set of samples initialized in the PCS space and its corresponding points in the same PCS after one round of color mapping. As a result, we will verify another color transformation from CIECAM02 to XYZ(CIELAB) and back to CIECAM02. $\bar{M}_{HPE}$ is adopted in both experiments. Moreover,

the symmetric extension of the post-adaptation nonlinearity as suggested by Moroney et.al. is adopted in this experiment [3]:

$$f(x) = 0.1 + sign(x)\frac{400(\frac{F_L|x|}{100})^{0.42}}{27.13 + (\frac{F_L|x|}{100})^{0.42}} \tag{13}$$

, where $x \in \{R', G', B'\}$. Therefore, we can derive the range:

$$-400 < (f(x) - 0.1) < 400. \tag{14}$$

Case 1: $CIELAB \rightarrow CIECAM02 \rightarrow CIELAB$

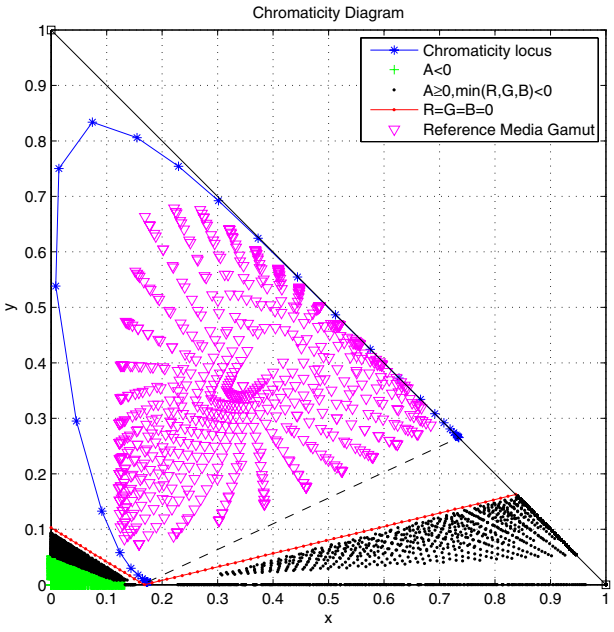

Figure 1. *Chromaticity diagram of Case 1 color transformation*

Various papers have been published addressing this approach [5, 7, 8]. The CIELAB color space is first projected to the nonnegative XYZ quadrant before mapping to CIEAM02. The necessary condition for the CIECAM02 forward model to succeed is that the achromatic response A is greater or equal to zero, where $A = (2R'_a + G'_a + \frac{1}{20}B'_a - 0.305)N_{bb}$. The sufficient condition for $A \geq 0$ is

$$\begin{aligned} \min\{R'_a, G'_a, B'_a\} \geq 0.1 \quad &\Leftrightarrow \quad \min\{R', G', B'\} \geq 0 \\ &\Leftrightarrow \quad \bar{M}_{HPE} \begin{pmatrix} X \\ Y \\ Z \end{pmatrix} \geq 0. \end{aligned} \tag{15}$$

We can construct the sufficient condition for valid CIECAM02 forward transformation using $\bar{M}_{HPE}$ in the chromaticity diagram as in [5, 6], and they can be represented as the following set of linear inequalities:

$$\begin{aligned} 0.468391x + 0.767661y &\geq 0.078684 \\ -0.27662x + 1.13699y &\geq -0.04641 \\ x + y &\leq 1 \\ x \geq 0 \quad , \quad y &\geq 0. \end{aligned} \tag{16}$$

They are equivalent to the analysis offered by Li and Luo except the slight difference at the first inequality because of the modified first row of the Hunt-Pointer-Estevez matrix [5]. Note that there exists samples for which $A > 0$ but $\min\{R', G', B'\} < 0$. Because of the adopted symmetric extension as Equation (13), the forward and backward CIECAM02 transformation are valid at these points.

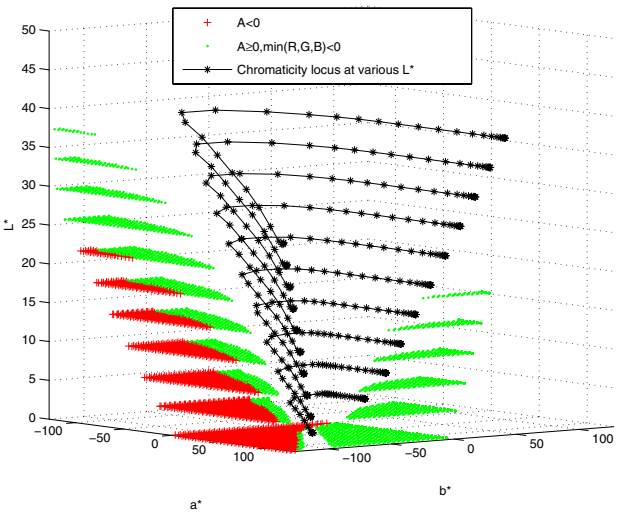

Figure 2. *CIELAB 3D graph of Case 1 color transformation*

Our numerical experiment indicates that both the standard CIECAM02 inverse model and our proposed model work, which means that no singular value truncation is needed in our proposed inverse model under this scenario. Moreover, the maximal roundtrip error in ΔE_{76} is 1.7×10^{-4}, which is slightly smaller than those reported in [5]. Figure 1 shows the chromaticity diagram of the chromaticity locus, chromaticity regions where $A < 0, A \geq 0$ but $\min\{R', G', B'\} < 0$, and the border where $R' = G' = B' = 0$. Figure 2 is the same result represented in the CIELAB color space. It is obvious that the entire chromaticity locus can be safely represented in the CIECAM02 color space even without the symmetric extension of the post-adaptation nonlinearity. This conclusion agrees with Li and Luo [5], but differs from that of Tastl et. al [7]. The four active constraints in (16) form a convex set denoted as S_c. Thus, any convex set with vertices inside S_c is contained in S_c. Therefore, we can conclude that any RGB color space with all primaries satisfying the set of linear inequality constraint (16) can be accurately represented in CIECAM02 color space . At last, the proposed reference media gamut as shown in Figure 1 also lies entirely within S_c [2, 7].

To verify the effect of singular value truncation, we adopt our TSVD-based inverse model with a lower threshold 0.1 for the computed singular value, and its result is shown in Figure 3. We can see that the singular value truncation algorithm automatically handles all imaginary colors within the CIECAM02 color space with $A < 0$. Figure 4 shows that same effect in the CIELAB 3D color space.

Case 2: $CIECAM02 \rightarrow XYZ(CIELAB) \rightarrow CIECAM02$

Unlike the first case where the unrealizable CIELAB points are projected to the nonnegative XYZ quadrant before applying

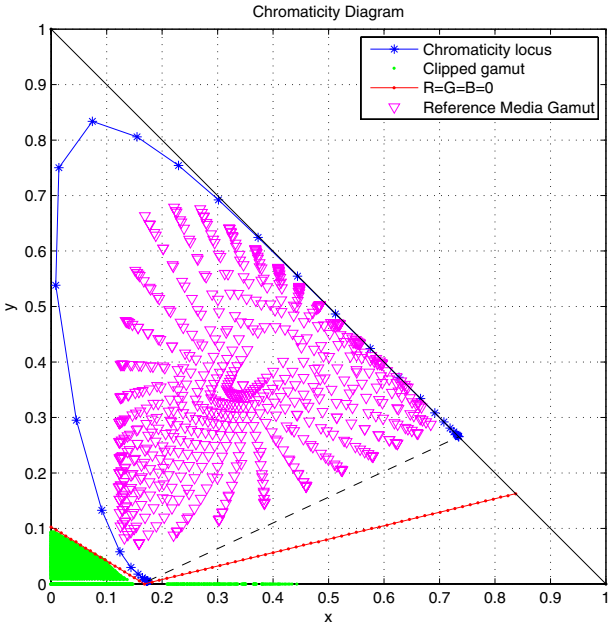

Figure 3. *Proposed TSVD inverse model effect in Chromaticity diagram*

the CIECAM02 forward transformation as suggested in the ICC specification [2], the entire CIECAM02 color cubic is mapped to XYZ color space before the projection can take place. Thus, this process will verify how the standard CIECAM02 inverse model and our proposed model handle imaginary colors. One constraint which is inactive in the first case is the range of the post-adaptation nonlinear response as listed in Equation (14). Therefore, a hard clipping function with the upper limit being 399 is imposed on $|R'_a|$, $|G'_a|$, and $|B'_a|$. Furthermore, when the standard CIECAM02 inverse model is used, the derived a and b for any point with chroma $C < 0.01$ will be set automatically to be zero to avoid numerical singularities. When our proposed inverse model is applied, a lower threshold of 0.1 is imposed on the singular values of the derived 3×3 matrix.

We first compare the computed $\{R'_a, G'_a, B'_a\}$ from the standard inverse model and the TSVD model. The range of the standard inverse model is from $\{-81.6, -1637.9, -10382.1\}$ to$\{1081.6, 108.5, 3806.7\}$, and that of the TSVD inverse model is from $\{-3.6, -5.0, -53.6\}$ to $\{14.4, 15.7, 77.5\}$, where the corresponding value of the adapted white point is $\{13.05, 13.05, 13.05\}$. It is obvious that the results reported by the standard algorithm are too large. Figure 5 and 6 demonstrate the result of the roundtrip color mapping. The TSVD inverse model automatically controls the output of the inverse function within a reasonable range while the standard inverse model is less robust against imaginary colors within the initial 3D grid points.

Conclusion

A constraint is first imposed on the CIECAM02 color appearance model such that the adapted white point should be perceived with zero chroma under complete illumination adaptation. Consequently, a modified Hunt-Pointer-Estevez matrix is derived in Equation (4). Furthermore, we propose a robust backward numerical implementation based on the TSVD algorithm,

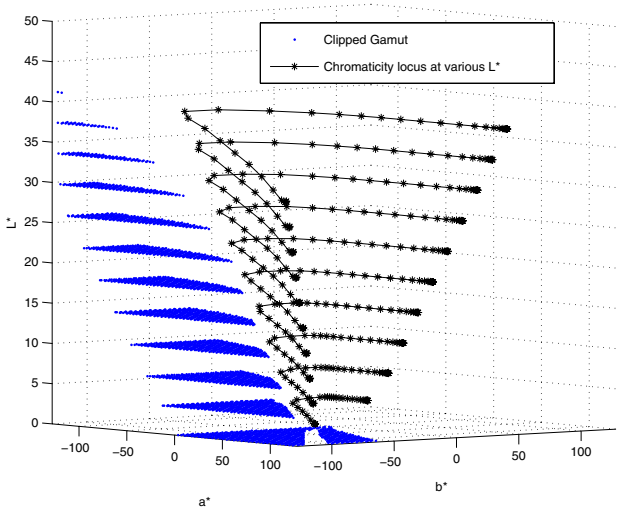

Figure 4. *Proposed TSVD inverse model effect in the CIELAB space*

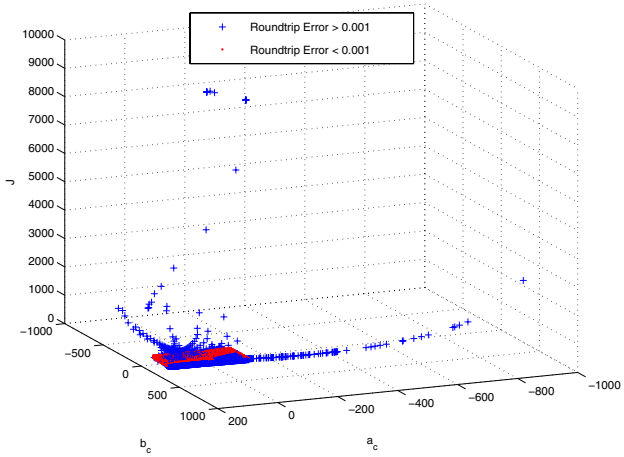

Figure 5. *Standard inverse model roundtrip effect in CIECAM02*

which addresses the potential numerical instability of the standard backward model. Two numerical experiments in the previous section indicate that both backward model implementations achieve high round-trip accuracy under the first $CIELAB \rightarrow CIECAM02 \rightarrow CIELAB$ experiment, where the $CIELAB$ color space is first mapped to the nonnegative quadrant of XYZ color space. However, the standard backward model suffers numerical instability in the second numerical experiment, $CIECAM02 \rightarrow CIELAB \rightarrow CIECAM02$, as shown in Figure 5, where unnaturally high lightness J results from this round-trip experiment. The TSVD-based backward model automatically controls the output within a reasonable range as shown in Figure 6 where the lower bound of the singular values is set to be 0.1. The numerical singularity at chroma of zero in the standard backward numerical algorithm is also avoided.

References

[1] Mark Fairchid, Color Appearance Models, 2nd Ed., Wiley-IS&T series in Imaging Science, 2005.

[2] International Color Consortium, Specification ICC.1:2004-10, Feb

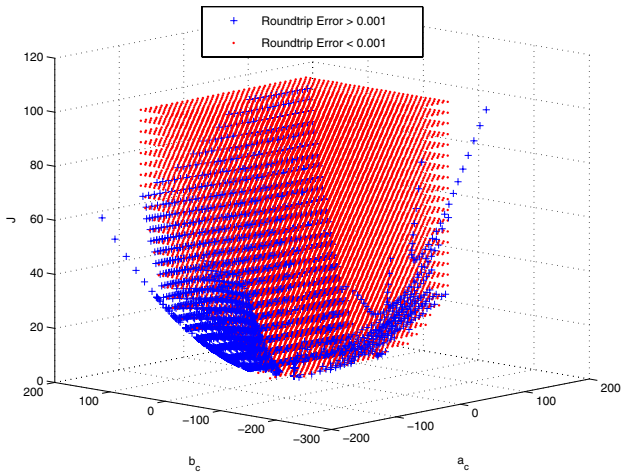

Figure 6. *Proposed TSVD inverse model roundtrip effect in CIECAM02*

2005.

[3] N. Moroney et. al., "The CIECAM02 Color Appearance Model", IS&T/SID Tenth Color Imaging Conference, pp. 23-27, 2002.

[4] N. Moroney and Z. Huan, "Field Trials of the CIECAM02 Color Appearance", CIE 25th Quadrennium, Feb 2003.

[5] C. Li and M. Luo, "Testing the Robustness of CIECAM02", Color Research and Application, pp. 99-106, Vol30, No2, April, 2005.

[6] M. Brill, "Irregularity in CIECAM02 and its Avoidance", Color Research and Application, pp. 142-145, Vol31, No2, APril, 2006.

[7] I. Tastl, M. Bhachech, N. Moroney, and J. Holm, "ICC Color Management and CIECAM02", IS&T/SID 13th Color Imaging Conference, pp. 217-223, Nov, 2005.

[8] R. Guay, M. Shaw, "Dealing with Imaginary Color Encodings in CIECAM02 in an ICC Workflow", IS&T/SID 13th Color Imaging Conference, pp. 318, Nov 2005.

[9] Per Christian Hansen, "Rank-Deficient and Discrete Ill-Posed Problems", SIAM, 1998.

Author Biography

Chunghui Kuo received his BS in Electrophysics at National Chiao-Tung University, a MS in Electrical Engineering at Ohio State University, and PhD in Electrical and Computer Engineering from University of Minnesota. He has been with the NexPress division of Eastman Kodak Company since 2001. His research interests are in areas of image processing, image quality, blind signal separation and classification, and neural networks that are applied in signal processing. He is a senior member of IEEE Signal Processing Society and a member of IS&T.

Eric K. Zeise is a Research Associate and Group Leader for Image Quality Evaluation in the NexPress division of Eastman Kodak Company in Rochester, NY. He received his BS in physics from the University of Massachusetts, and MS and PhD degrees in low-temperature physics from Cornell University. He holds 19 patents in the areas of systems modeling, printing systems architecture, and perceptual image quality evaluation. Eric is a member and contributor to IS&T, IEEE, and APS, and has been invited to give several tutorials in the areas of image quality, color printing, and color management. He is active in standards development as Project Editor for the ISO/IEC JTC-1 SC28 and INCITS W1.1 team developing appearance-based image quality standards for printers and is Convenor of the ISO/IEC JTC-1 SC28 Working Group 4 (Image Quality).

Di Lai received his BS in Biomedical Electronic Engineering at Xi'an Jiaotong University and a MS from the Center for Imaging Science at the Rochester Institute of Technology in 1999. His research interests are in image processing, color science, and 3D visualization. He joined the NexPress division of Kodak in 1999 as an Imaging Scientist. He has been an IEEE member since 2003.